

Supplementary Data

Dynamic 23S rRNA modification by ho⁵C2501 benefits *Escherichia coli* under oxidative stress

Michel Fasnacht,^{1,2} Stefano Gallo,^{1,2} Puneet Sharma,¹ Maximilian Himmelstoß,⁴ Patrick A. Limbach,³ Jessica Willi,^{1,2,3,†,*} and Norbert Polacek^{1,*}

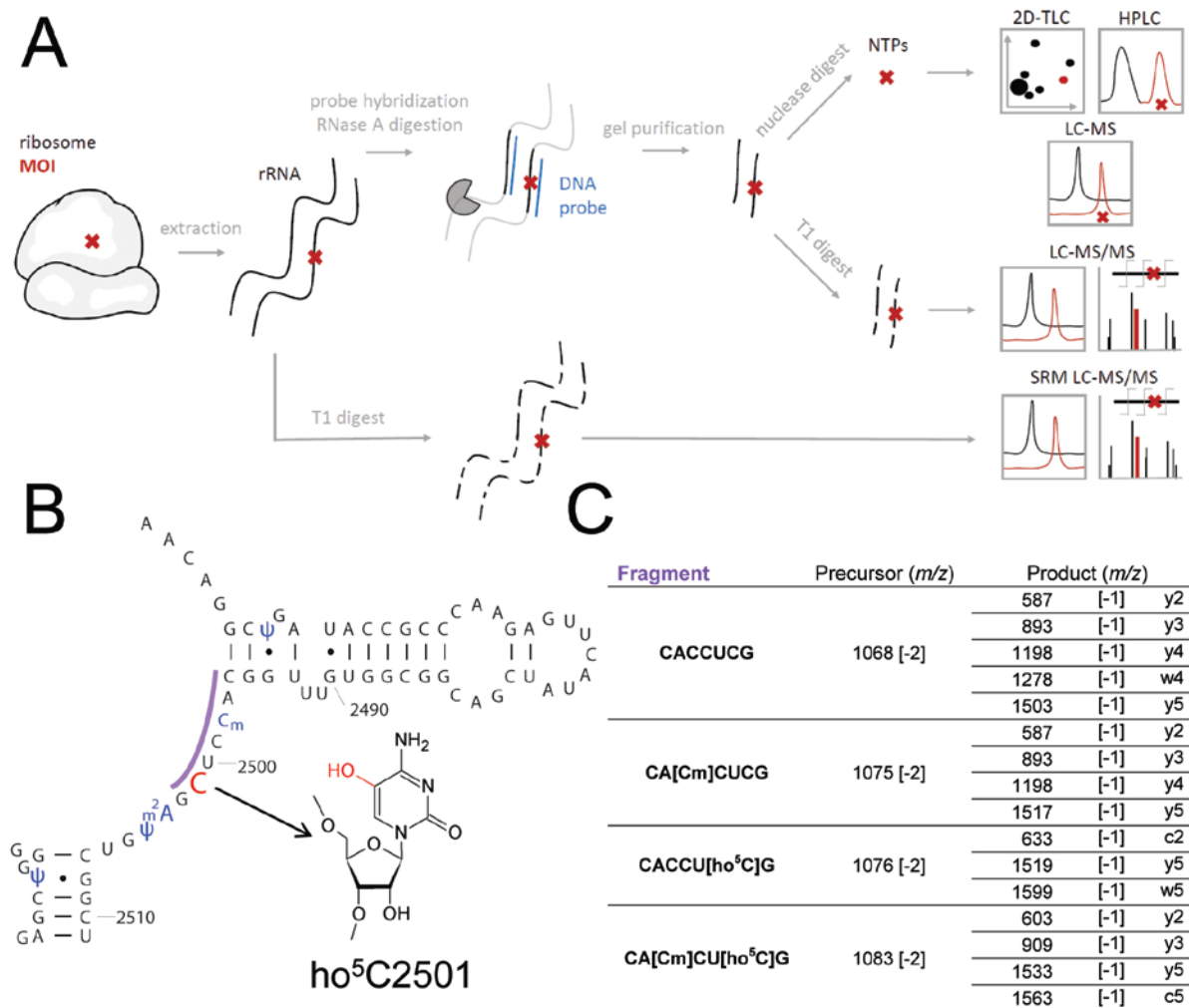
¹ Department of Chemistry, Biochemistry and Pharmaceutical Sciences, University of Bern, 3012 Bern, Switzerland

² Graduate School for Cellular and Biomedical Sciences, University of Bern, 3012 Bern, Switzerland

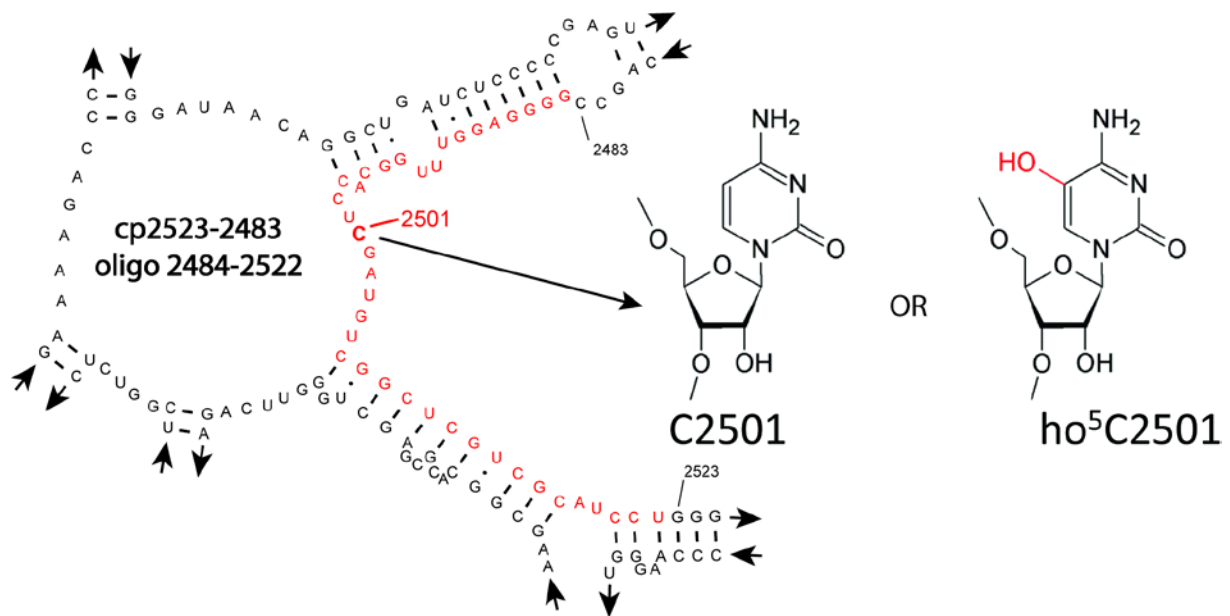
³ Rieveschl Laboratories for Mass Spectrometry, Department of Chemistry, University of Cincinnati, Ohio, USA

⁴ Institute of Organic Chemistry, Center for Molecular Biosciences Innsbruck, University of Innsbruck, 6020 Innsbruck, Austria

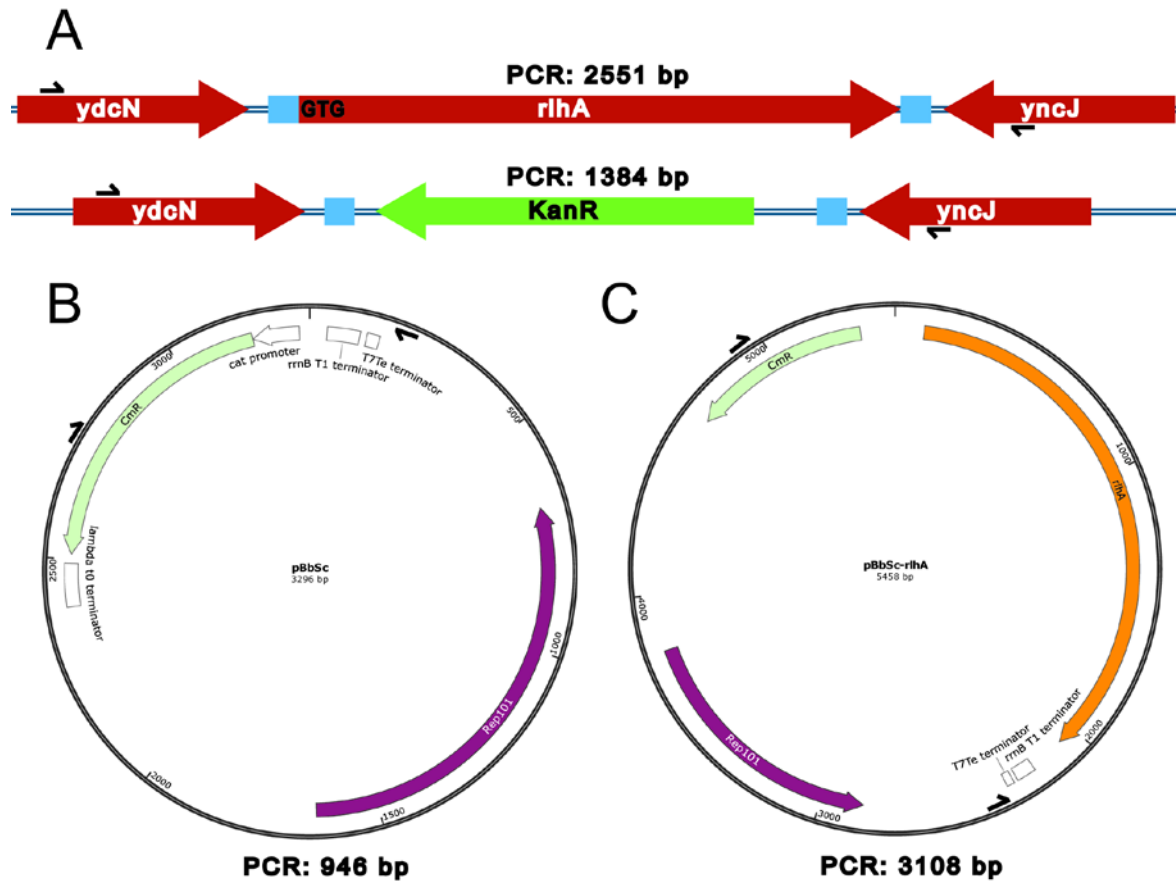
Supplementary Figures



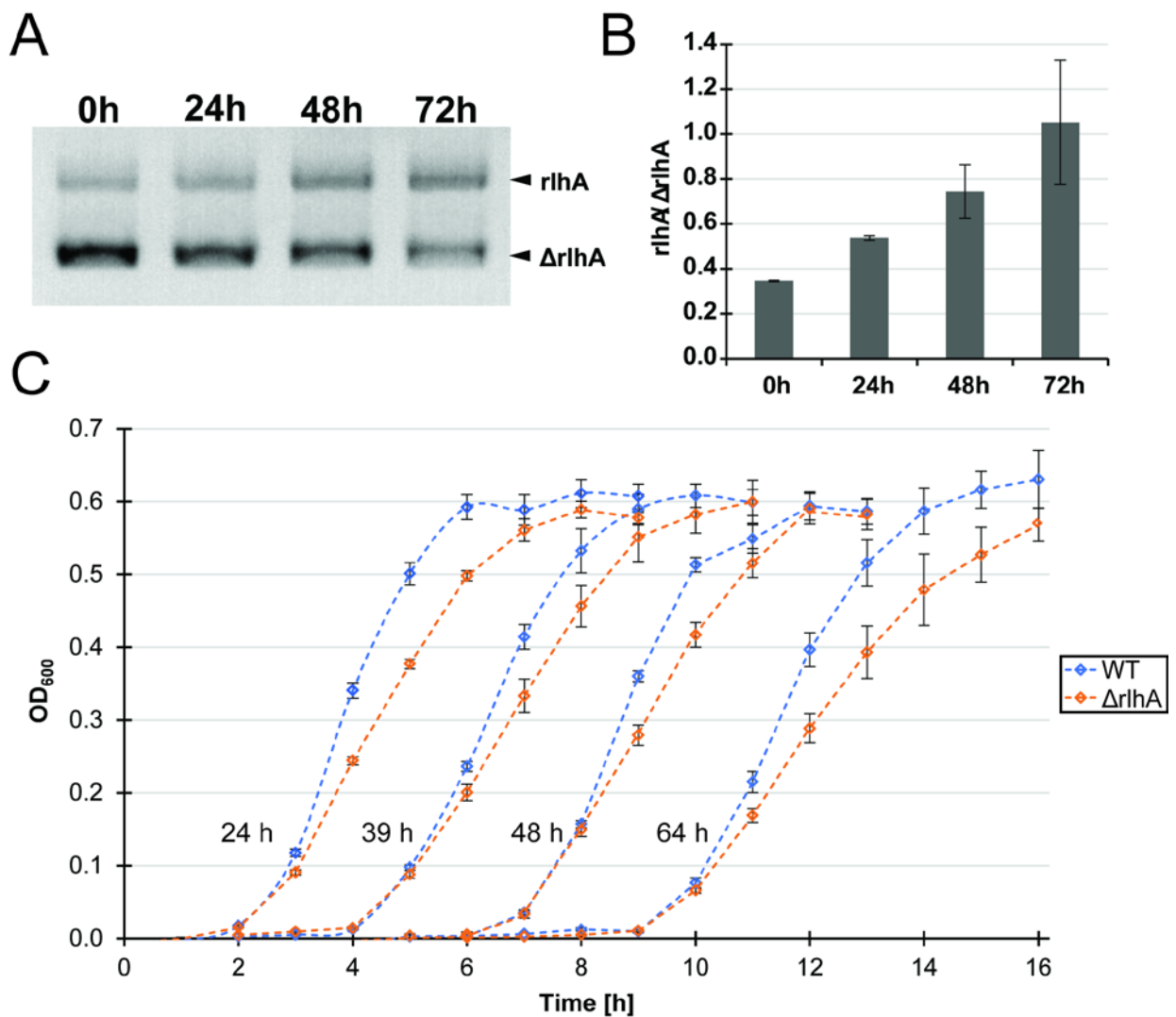
Supplementary Figure S1. (A) Previously published methods for ribosomal RNA modification (red cross) measurements included a DNA oligo protected RNase A digestion step to remove regions of no interest (top). Afterwards, the undigested residual RNA oligo was isolated and digested to nucleoside triphosphate size (NTPs) or to smaller fragments with RNase T1, which cuts after every guanine. The resulting fragments or NTPs were then analyzed by thin layer chromatography (TLC), liquid chromatography (LC) or mass spectrometry (MS) methods. For our analysis of hydroxylation at position C2501, we directly digested the isolated 23S rRNA by RNase T1 and analyzed the resulting fragments by LC-MS/MS run in single reaction monitoring (SRM) mode. **(B)** Excerpt of the two-dimensional structure of *E. coli* 23S rRNA with known post-transcriptional modifications marked in blue. The resulting fragment of interest (C2496-G2502) after RNase T1 digestion is marked in violet. Adapted from <http://www.rna.icmb.utexas.edu> **(C)** Potential precursor mass from different fragment possibilities with C2498 and C2501 modified or not. Additionally, the mass of different product ions is given according to the product type. Charge states are indicated in square brackets.



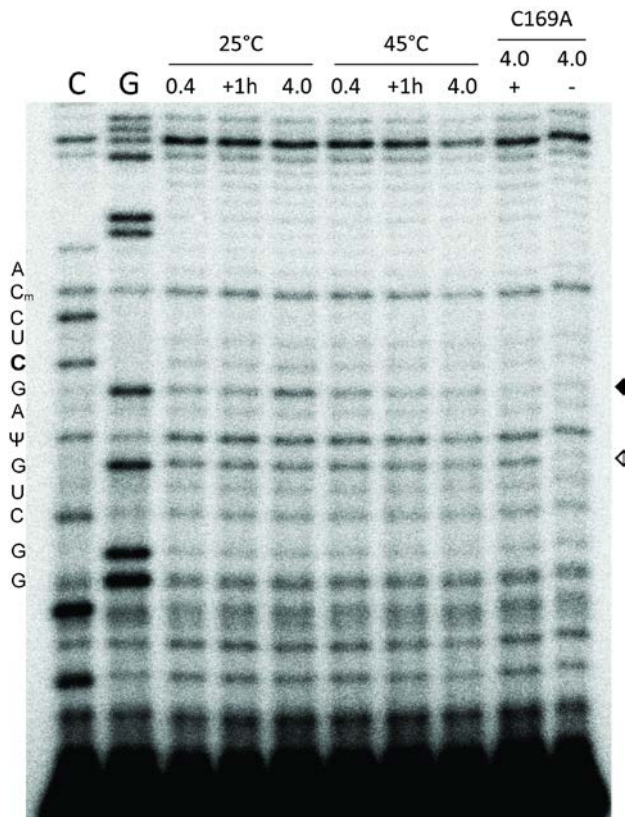
Supplementary Figure S2. Central loop of domain V shows the circular permutation of 23S rRNA to cp2523-2483 (named after its new 5' and 3' ends, indicated), filled with the synthetic RNA oligo compensating residues 2484-2522 (red), and carrying either C or ho⁵C in position 2501. The RNA fragment base pairs to the cp-23S during *in vitro* reconstitution.



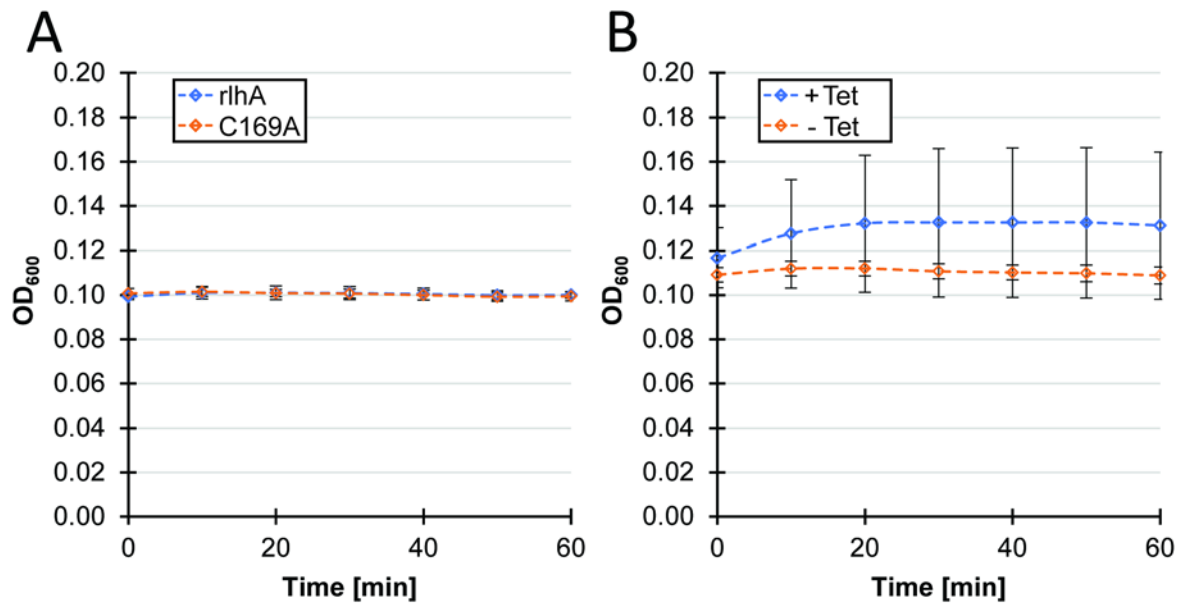
Supplementary Figure S3. (A) Genomic locus of *rhlA* before and after replacement by a kanamycin resistance cassette. Blue boxes represent 40 base pairs long homologous regions used for recombination. The homologous regions were designed to be 40 bp up- and downstream of the start and stop codon, respectively, completely removing the *rhlA* sequence on the chromosome upon recombination. Black arrows indicate binding sites for primers to control the genomic locus by PCR. **(B)** Empty plasmid vector backbone encoding for a chloramphenicol resistance (CmR) and **(C)** cloned complementation plasmid with the *rhlA* genomic region with 100 bp up- and downstream extension inserted by PIPE. Black arrows indicate binding sites for primers to control plasmids by PCR. Plasmid maps were generated in SnapGene Viewer.



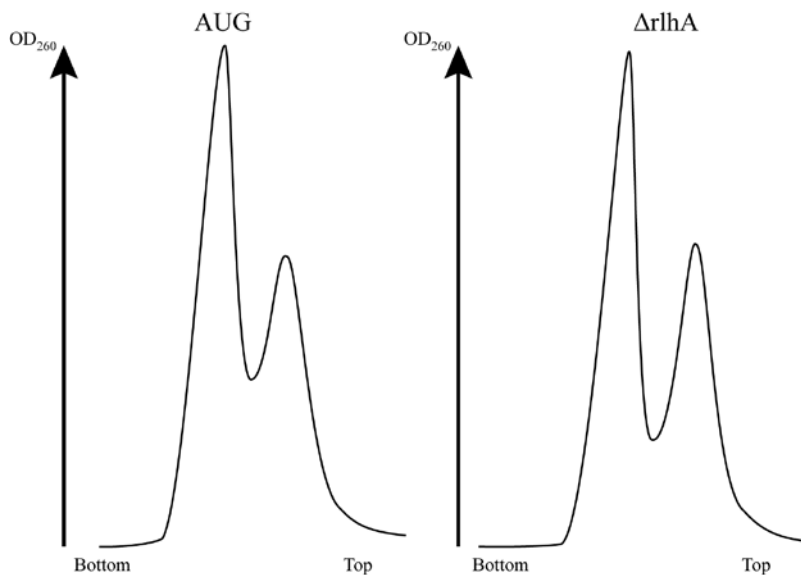
Supplementary Figure S4. (A) PCR on the plasmid insert region to control for the amount of complementation (*rIhA*) and Δ *rIhA* knockout strain after repeated 24 h incubation at 37°C, starting with an initial 1:1 mixture of both strains (0 h). As can be seen in the initial 1:1 mixture (0 h), the PCR reaction preferably amplified the shorter product corresponding to the empty pBbSc vector of the Δ *rIhA* strain. Nevertheless a clear growth competition in favor of the *rIhA* strain was apparent. (B) Average ratio of complementation over knockout strain was calculated with the quantification of PCR signals observed in (A), error bars represent standard deviation (n = 2). (C) Recovery from stationary phase was analyzed in wildtype (WT) and *rIhA* knockout (Δ *rIhA*) cells by recording growth in a 96 well plate under unstressed conditions by simultaneous re-dilution of 24–64 h post-inoculum cultures in fresh LB medium.



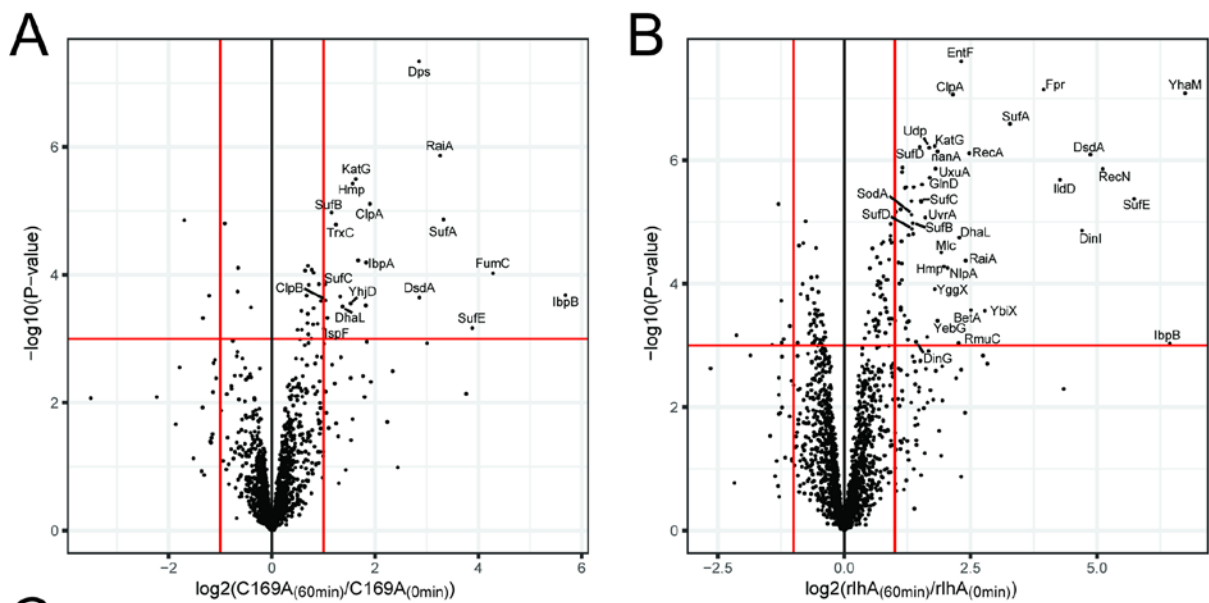
Supplementary Figure S5. Representative 15% polyacrylamide gel with cDNA generated from CMCT treated and hydrolyzed total RNA samples isolated from unstressed wildtype *E. coli* cells in exponential phase ($OD_{600} = 0.4$) and one hour after the addition of the specified stress (+1 h). An additional sample was taken once the cultures reached stationary phase under the specified stress conditions ($OD_{600} = 4.0$). For the ho⁵C2501-lacking C169A strain both a CMCT treated (+) and buffer only (-) control are shown with total RNA isolated from stationary phase. C and G are dideoxy-sequencing lanes that were prepared with untreated total RNA. Two others naturally occurring rRNA modifications are indicated (Cm2498 and Ψ2504), while position C2501 is marked in bold. A black arrowhead marks the expected site of the ho⁵C2501 stop upon CMCT-treatment and the open arrowhead shows the stop corresponding to Ψ2504.



Supplementary Figure S6. (A) Average OD₆₀₀ over the course of one hour of three biological replicates of *rlhA* (blue) and C169A (orange) strains after the addition of 5 mM H₂O₂ at t = 0. OD₆₀₀ was measured in a 96 well plate in the Tecan M1000 PRO plate reader. Error bars indicate standard deviation. **(B)** Same as in A, but using the C169A + *dps* strain in the absence (- Tet) or presence (+ Tet) of ectopic *dps* overexpression.

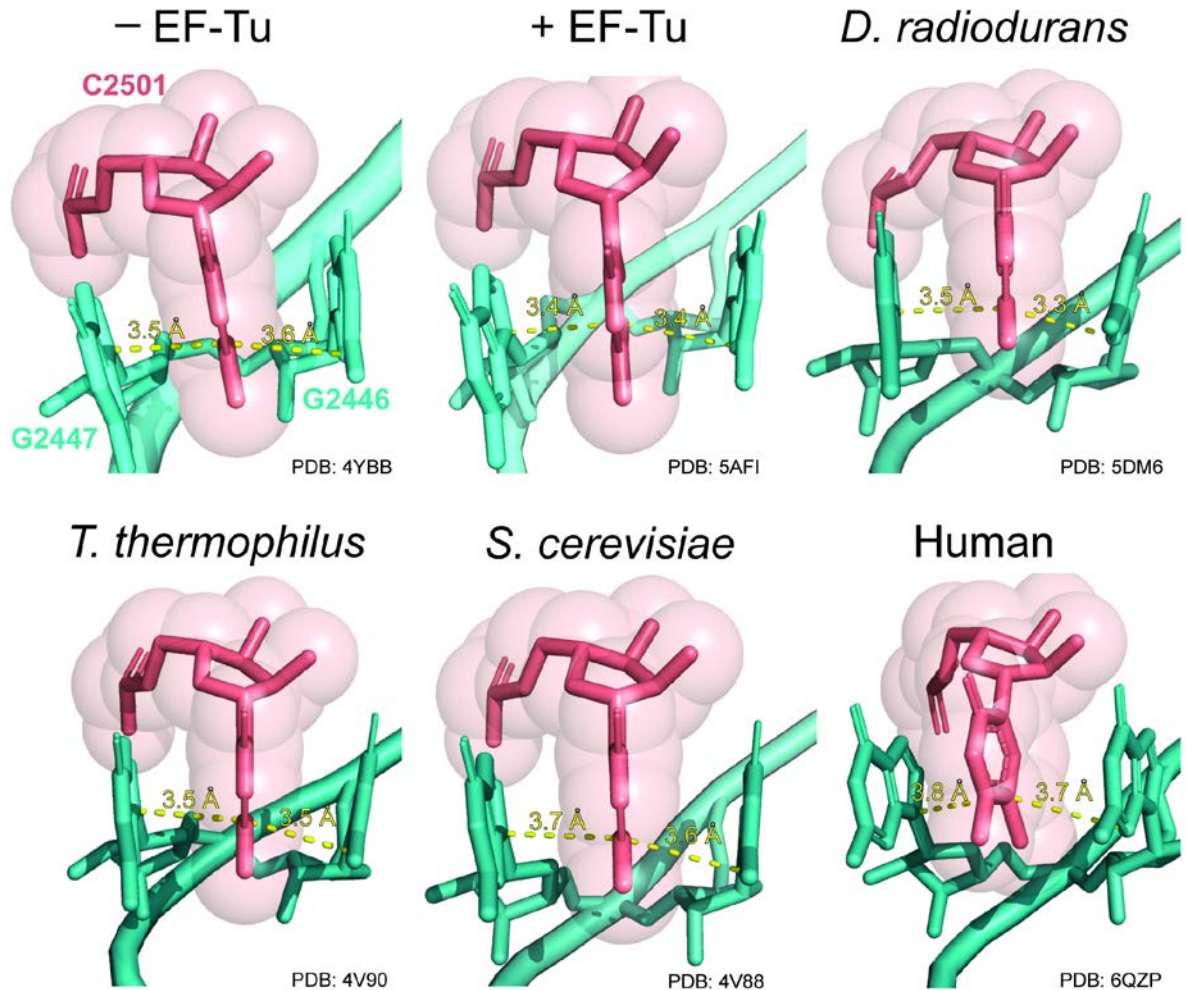


Supplementary Figure S7. Sucrose density gradient profile obtained by OD₂₆₀ absorbance tracing during ribosomal subunits isolation from both the AUG and Δ *rlhA* strain (left peak: 50S subunits, right peak: 30S subunit). No obvious differences in the subunit ratios between the two strains were apparent thus excluding gross ribosome biogenesis defects in the Δ *rlhA* strain.

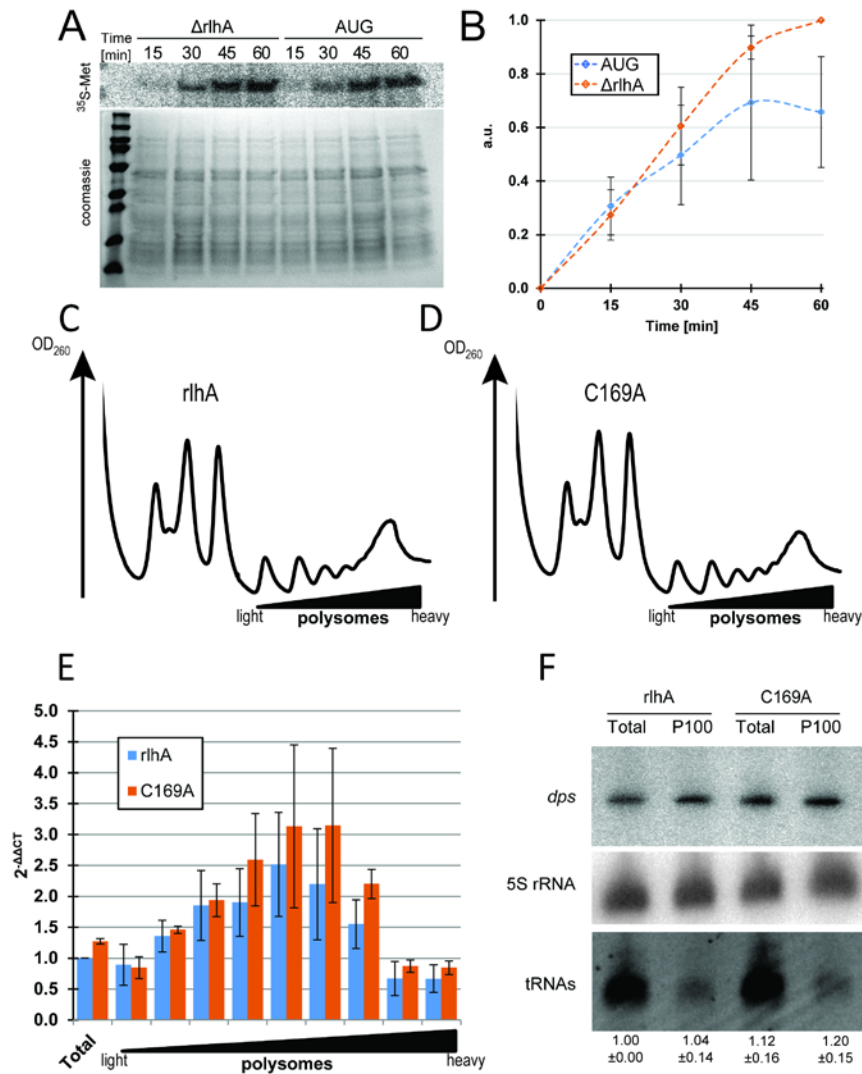


GO biological process complete	Escherichia coli - REFLIST (4390)	C169A (22)	C169A (fold Enrichment)	C169A (raw P-value)	C169A (FDR)
iron-sulfur cluster assembly (GO:0016226)	21	5	47.51	1.16E-07	1.86E-04
metallo-sulfur cluster assembly (GO:0031163)	21	5	47.51	1.16E-07	1.24E-04
response to oxidative stress (GO:0006979)	101	6	11.85	9.62E-06	6.14E-03
response to temperature stimulus (GO:0009266)	85	5	11.74	6.33E-05	3.36E-02
response to stress (GO:0006950)	557	14	5.02	3.76E-08	1.20E-04
response to stimulus (GO:0050896)	930	15	3.22	3.06E-06	2.44E-03
GO biological process complete	Escherichia coli - REFLIST (4390)	rhA (79)	rhA (fold Enrichment)	rhA (raw P-value)	rhA (FDR)
mannose transmembrane transport (GO:0015761)	3	3	55.57	1.02E-04	1.63E-02
N-acetylglucosamine transport (GO:0015764)	4	3	41.68	1.77E-04	2.26E-02
hexose import across plasma membrane (GO:0140271)	4	3	41.68	1.77E-04	2.17E-02
glucose import across plasma membrane (GO:0098708)	4	3	41.68	1.77E-04	2.09E-02
carbohydrate import across plasma membrane (GO:0098704)	4	3	41.68	1.77E-04	2.01E-02
fructose import (GO:0032445)	5	3	33.34	2.79E-04	2.87E-02
L-alanine metabolic process (GO:0042851)	5	3	33.34	2.79E-04	2.78E-02
glucose import (GO:0046323)	6	3	27.78	4.14E-04	3.88E-02
D-amino acid metabolic process (GO:0046416)	10	4	22.23	7.92E-05	1.33E-02
iron-sulfur cluster assembly (GO:0016226)	21	7	18.52	3.62E-07	1.93E-04
metallo-sulfur cluster assembly (GO:0031163)	21	7	18.52	3.62E-07	1.65E-04
tricarboxylic acid cycle (GO:0006099)	29	7	13.41	2.28E-06	7.27E-04
SOS response (GO:0009432)	30	6	11.11	3.22E-05	6.03E-03
aerobic respiration (GO:0009060)	54	8	8.23	1.04E-05	2.56E-03
response to oxidative stress (GO:0006979)	101	10	5.5	2.04E-05	4.33E-03
sulfur compound metabolic process (GO:0006790)	126	10	4.41	1.18E-04	1.79E-02
small molecule catabolic process (GO:0044282)	297	20	3.74	3.22E-07	3.42E-04
carboxylic acid catabolic process (GO:0046395)	186	12	3.59	1.53E-04	2.12E-02
organic acid catabolic process (GO:0016054)	195	12	3.42	2.33E-04	2.48E-02
organonitrogen compound catabolic process (GO:1901565)	202	12	3.3	3.18E-04	3.07E-02
cellular response to DNA damage stimulus (GO:0006974)	270	16	3.29	2.83E-05	5.65E-03
response to stress (GO:0006950)	557	33	3.29	2.03E-10	6.48E-07
cellular response to stress (GO:0033554)	377	21	3.1	3.00E-06	8.70E-04
cellular catabolic process (GO:0044248)	383	21	3.05	3.82E-06	1.02E-03

Supplementary Figure S8. (A) Volcano plot of the comparative proteome analysis of 60 minutes 2 mM H₂O₂ stressed C169A cells versus unstressed, exponentially growing C169A cells. A fold-change of at least +/-2 is indicated by vertical red lines crossing the x-axis at +/-1, respectively. The p-value cut-off of 0.001 is indicated by a horizontal red line (n = 3). **(B)** Volcano plot as in (A), but displaying the comparison of expressed proteins in stressed and unstressed rhA cells (n = 3). **(C)** Gene ontology (GO) term analysis of the significantly up- and downregulated proteins under stressed conditions in both (A) and (B). The analysis was performed using the PANTHER overrepresentation test (1). Significance was calculated using Fisher's exact test and the false discovery rate (FDR) was calculated as correction.



Supplementary Figure S9. Conserved three-dimensional structural arrangement of C2501 in *E. coli* and the corresponding nucleotide in the specified species (red with transparent spheres). For *E. coli*, two structures with either resting (-EF-Tu) or actively translating (+EF-Tu) ribosomes are shown. In all organisms and conditions, the C2501 nucleotide is base-stacked between two guanosines (teal). Distance measurement of the C5 of C2501 to the N9 of G2447 (left) and to the N3 of G2446 (right) are indicated in yellow. Note that in both *S. cerevisiae* (not visible) and in human ribosomes the C5 of the corresponding C2501 nucleotide carries a methylation.



Supplementary Figure S10. (A) Representative phosphorimager scan of *in vitro* translated ³⁵S-labelled *dps* protein (top) and coomassie stained proteins as loading control at the bottom. *In vitro* translations were performed with ribosomes carrying 50S subunits isolated from an unmodified knockout strain (Δ rlhA) and an almost stoichiometrically modified strain (AUG). (B) Quantification of average signal intensities at the marked time points with the signal intensity of Δ rlhA (t = 60 min) set to 1. Error bars indicate standard deviation (n = 3). (C) & (D) Representative 10-50% sucrose gradient profiles recorded at 260 nm with whole cell lysates isolated from the complementation strain rlhA and the inactive mutant strain C169A. Fractions for RNA isolation were collected from the light to heavy polysomes region. (E) Enrichment of the *dps* mRNA in the isolated polysomal RNA fractions from (C) and (D) compared to the total RNA isolation of each strain was analyzed by qRT-PCR. Displayed are the mean $2^{-\Delta\Delta CT}$ values, error bars indicate standard deviations (n = 3). (F) Representative northern blot analysis of *dps* mRNA in both total RNA and P100 RNA samples. Northern blot analysis of the 5S rRNA served as a loading control. Ethidium bromide staining of tRNAs in the 4% polyacrylamide gel is shown to prove enrichment of the ribosomal particles in the P100. At the bottom, average signal intensities of the *dps* mRNA are shown including the standard deviation range. *dps* mRNA signal intensity in the total RNA samples isolated from the rlhA replicates were set as 1 (n = 3).

Supplementary Methods

Polysome Profiling and RT-qPCR

The cells of 80 ml cultures of exponentially growing rlhA and C169A strains ($OD_{600} \sim 0.4$) were harvested by quick vacuum filtration through a mixed cellulose ester membrane (*Whatman* ME25, Φ 0.45 μm) and immediately shock frozen together with 500 μl of 1x TMN (50 mM Tris-HCl, pH 7.6, 100 mM NH_4Cl , 10 mM MgCl_2 , 6 mM β -mercaptoethanol) in liquid N_2 . Cells were then opened under cryogenic conditions using a SPEX SamplePrep freezer-mill (2 cycles of 2 min at 5 CPS with 2 min of cooling in between). The lysed samples were then thawed on ice with an additional 250 μl of 1x TMN added. Next, cell debris was removed by two centrifugation steps at 4°C (5,000 xg, 3 min and 10,000 xg, 5 min) and the OD_{260} of the cleared lysate was measured on NanoDrop (*Thermo Scientific*). A total of 8 OD_{260} units were then loaded and separated on 10-50% sucrose gradients in 1x TMN at 35,000 rpm for 3 h at 4°C (SW 41 Ti rotor from *Beckman Coulter*), whereas total RNA was isolated from the remaining cell lysate using hot acid phenol extraction. The gradients were finally fractionated and RNA from the polysomal fractions was isolated according to reference (2). *dps* mRNA levels in both the total and polysomal RNA fractions was determined by RT-qPCR according to previously published protocols (3). *gyrA* was used as a reference gene throughout. Used primers can be found in **Supplementary Table S1**.

Supplementary References

1. Mi, H., Ebert, D., Muruganujan, A., Mills, C., Albu, L.P., Mushayamaha, T. and Thomas, P.D. (2021) PANTHER version 16: A revised family classification, tree-based classification tool, enhancer regions and extensive API. *Nucleic Acids Res.*, **49**, D394–D403.
2. Nedialkova, D.D. and Leidel, S.A. (2015) Optimization of Codon Translation Rates via tRNA Modifications Maintains Proteome Integrity. *Cell*, **161**, 1606–1618.
3. Raad, N., Luidalepp, H., Fasnacht, M. and Polacek, N. (2021) Transcriptome-Wide Analysis of Stationary Phase Small ncRNAs in *E. coli*. *Int. J. Mol. Sci.*, **22**, 1703.